Results in Nonlinear Analysis 8 (2025) No. 3, 59–81 https://doi.org/10.31838/rna/2025.08.03.003 Available online at www.nonlinear-analysis.com



Results in Nonlinear Analysis

Peer Reviewed Scientific Journal

A comprehensive extended SEIR model for hMPV transmission: Integrating co-infection and vaccination dynamics for Türkiye's model

Aytekin Enver^a, Fatma Ayaz^a, Ali M. O. A. Anwer^b, Reyhan Bilgic Ak^c

^aDepartment of Mathematics, Gazi University, Ankara, Türkiye; ^bTechnical College of Management, Northern Technical University, Ninevah, Iraq; ^cGraduate School of Natural and Applied Sciences, Gazi University, Ankara, Türkiye

Abstract

Human metapneumovirus (hMPV) is a common respiratory virus that represents a major public health burden, especially in children, older adults, and immunocompromised patients. However, traditional compartmental models, which apply to single-pathogen transmission, do not always adequately characterize the complexity of co-infections and vaccination dynamics. Here, we extend a SEIR model with two more compartments: one for those coinfected with hMPV, one for those infected with respiratory viruses other than hMPV, and another compartment for the vaccinated. This complex frame allows a realistic representation of hMPV transmission and control interventions. As a numerical solution method, we use the finite difference method (FDM) to study the behavior of these nonlinear and coupled differential equations. This method breaks down the time evolution of each compartment and can be used to simulate disease dynamics under different public health intervention schemes, such as vaccination rates. Simulation shows that intensive vaccination would significantly decrease the peak of infections and expedite the epidemic's control, especially together with non-pharmaceutical interventions. The co-infection compartment shows how the simultaneous presence of overlapping infections can exacerbate the severity of an epidemic, emphasizing the need for combined control strategies. Our model is a useful tool for understanding hMPV epidemic in the presence of other pathogens, which helps estimate the efficacy of vaccination strategies. This biologically motivated model, coupled with a strong numerical solution, provides important information for health authori-

Email addresses: aytekinanwer@gmail.com (Aytekin Enver), fayaz@gazi.edu.tr (Fatma Ayaz), alimahmoodoguranwer.anwer@gazi.edu.tr (Ali M. O. A. Anwer), reyhan.ak@gazi.edu.tr (Reyhan Bilgic Ak)

ties in their quest to minimize the effects of the disease. The extended SEIR framework demonstrates how vaccination intensity directly affects epidemic duration, recovery rates, and co-infection outcomes. Moreover, the scenario-based simulations highlight that aggressive vaccination strategies can reduce epidemic control time from nearly two months to less than three weeks, providing actionable insights for policymakers.

Mathematics Subject Classification (2010): 93A30, 65M06, 65L06, 32G34

Key words and phrases: Human metapneumovirus (hMPV); Mathematical Modeling; Finite Difference Method; Co-infection Dynamics; Vaccination Strategies

1. Introduction

Human metapneumovirus (hMPV), which was discovered in 2001, is now known as one of the most critical viral etiologic agents in acute respiratory infections, especially in young children, immuno-compromised patients, and elderly people [1]. The majority of infected cases are asymptomatic or present with mild to moderate symptoms; however, rare cases with severe clinical outcomes and complications also occur in patients who also suffer from comorbid conditions [2].

Traditional compartmental models, such as the SEIR (Susceptible–Exposed–Infectious–Recovered) framework, have been widely used to understand the dynamics of infectious diseases. These models provide a solid foundation for analyzing the fundamental mechanisms of disease spread. However, they often operate under simplifying assumptions, focusing on single pathogens and neglecting important real-world complexities such as co-infections and vaccination. Many clinical reports have confirmed that patients frequently harbor more than one respiratory pathogen simultaneously, which may intensify disease severity and alter transmission patterns. Ignoring such interactions can underestimate the scale of outbreaks and reduce the accuracy of predictive models.

In addition, vaccination remains one of the most effective public health measures for controlling epidemics, yet its impact is not always integrated into standard SEIR-type models. Incorporating vaccination dynamics alongside co-infection processes can provide a more realistic and comprehensive picture of epidemic trajectories, thereby improving the design of control strategies.

In this study, we extend the classical SEIR model by introducing additional compartments to represent co-infections with hMPV, infections with other respiratory viruses, and vaccinated individuals. This extension allows us to analyze overlapping infections and evaluate vaccination strategies within a unified framework. The model is solved numerically using the finite difference method (FDM), which enables accurate simulation of nonlinear and coupled dynamics. Simulation results show that intensive vaccination can significantly reduce the infection peak and shorten epidemic duration, particularly when combined with non-pharmaceutical interventions. Moreover, the co-infection compartment highlights how overlapping infections exacerbate epidemic severity, underscoring the importance of integrated control measures.

Human metapneumovirus (hMPV) is a leading cause of acute respiratory tract infections world-wide, particularly in children, older adults, and immunocompromised populations. Despite its clinical importance, mathematical modeling efforts for hMPV have been relatively limited compared to other respiratory viruses such as influenza or respiratory syncytial virus (RSV). This gap underscores the need for models that can capture both the biological characteristics of hMPV and the epidemiological complexity associated with its transmission.

Traditional SEIR-based models provide a valuable framework for understanding epidemic dynamics; however, they often focus on single-pathogen scenarios and neglect crucial factors such as co-infections and vaccination. In real-world settings, patients frequently present with multiple respiratory viruses at the same time, which can intensify disease severity and alter transmission pathways. Furthermore, vaccination strategies are increasingly being explored as essential tools in epidemic control, yet their effects are not always integrated into standard SEIR models. Addressing these gaps provides the motivation for the present study.

By extending the SEIR framework with compartments for co-infection and vaccination, we aim to more realistically represent hMPV epidemic dynamics. This approach not only allows for the analysis of overlapping infections and intervention strategies but also creates a platform to explore policy-relevant scenarios. In addition, the use of a robust numerical method, namely the finite difference method (FDM), ensures that the model can capture nonlinear behaviors and provide reliable simulations of epidemic evolution.

By extending the SEIR framework with compartments for co-infection and vaccination, we aim to more realistically represent hMPV epidemic dynamics. This approach not only allows for the analysis of overlapping infections and intervention strategies but also creates a platform to explore policy-relevant scenarios. In addition, the use of a robust numerical method, namely the finite difference method (FDM), ensures that the model can capture nonlinear behaviors and provide reliable simulations of epidemic evolution.

1.1. Epidemiological Relevance of hMPV

Epidemiologic data have revealed that hMPV is endemic worldwide and contributes to the seasonal load of respiratory illness [2–4]. It commonly circulates together with other respiratory viruses such as respiratory syncytial virus (RSV) and influenza, making the situation even harder for clinicians and public health authorities [5]. This overlapping circulation, as well as making the diagnosis of the individual viruses more difficult, also makes it prone to lead to more severe disease in the case of a double infection [6]. Interestingly, it has been reported that hMPV strains of multiple lineages co-circulate, and that this diversity could likely result in the widespread occurrence of hMPV in countries with high burden of importance, though a recent genotyping and molecular detection study from India has reported multiple co-circulating hMPV sublineages infecting the SARI patients [7].

1.2. Limitations of Traditional SEIR Modeling

SEIR (Susceptible—Exposed—Infectious—Recovered)-based compartmental models have been of particular importance for understanding the basic elements that govern the spread of respiratory viruses. These models, however, are often focused on a single pathogen and fail to adequately incorporate real-world complexities such as co-infections and vaccine strategies [8]. As many reports now show that individual patients may harbor more than one pathogen at a given time [3, 4], ignoring co-infection dynamics can underestimate both total infections and the extent of outbreaks.

To provide a clearer foundation for the subsequent model extension, we briefly present the classical SEIR model in its standard mathematical formulation. The model divides the total population N(t) into four compartments: Susceptible S(t), Exposed E(t), Infectious I(t), and Recovered R(t). The system is governed by the following set of ordinary differential equations:

$$\frac{dS}{dt} = -\beta \, \frac{SI}{N},\tag{1.1}$$

$$\frac{dE}{dt} = \beta \frac{SI}{N} - \sigma E,\tag{1.2}$$

$$\frac{dI}{dt} = \sigma E - \gamma I,\tag{1.3}$$

$$\frac{dR}{dt} = \gamma I. \tag{1.4}$$

Where

• β : transmission rate,

- σ : rate at which exposed individuals become infectious (inverse of incubation period),
- γ: recovery rate,
- N = S + E + I + R: total population (assumed constant).

This baseline model captures the dynamics of a single-pathogen outbreak but does not account for important factors such as co-infections with other viruses or the protective impact of vaccination. Therefore, in this study, we extend this framework by adding compartments for vaccinated and co-infected individuals to more accurately model the spread and control of hMPV in realistic scenarios.

1.3. Emerging Lineages and Geographic Distribution

Active genomic surveillance has identified new hMPV lineages that may change the transmissibility and immune evasion properties of the virus. To give you an example, N. Devanathan et al. (2025) reported the appearance of new hMPV sublineages A2.2.1 and A2.2.2 among pediatric cohorts from India, suggestive of their potential role in altering transmission dynamics and severity of disease [9]. Similarly, Zhu et al. (2020) found that co-infections of hMPV with parainfluenza virus might worsen clinical outcomes in high-risk groups, particularly elderly patients [10].

1.4. Pediatric Settings and Seasonal Dynamics

Several studies have concentrated on daycare centers and pediatric wards, where young children are especially susceptible to co-circulating viral pathogens [11]. Mendes et al. [12] have demonstrated that hMPV-rhinovirus co-infections may enhance both transmissibility and clinical severity, particularly in crowded indoor settings. Phases of seasonal peaks, often in late fall and winter, tend to coincide with a circulation of other respiratory viruses, thus fueling clusters of co-infection. Thus, prompt testing, strong vaccination strategies, and effective non-pharmaceutical measures (e.g., hand hygiene, wearing the correct mask, and enhanced ventilation) might together help mitigate the occurrence of severe co-infections.

However, viral infections such as hMPV continue to present challenges in treating patients, and emerging cell-based therapies hold promise for addressing these infections in innovative ways. By harnessing engineered immune cells to augment pathogen-specific immunity, virus-specific T-cell (VST) therapies have shown substantial promise in targeting viruses that are resistant to immune responses. They, including autologous or allogeneic T cells, have all shown promising pre-clinical activity in the context of respiratory viruses such as hMPV and RSV. In addition, the implementation of cellular therapies such as CAR T cells provides a novel modality to treat severe and co-infected cases of viral diseases in which vaccines and antiviral drugs do not work well. This highlights the need for further studies on cell-based immunotherapy as the mainstay of treatment for such elaborate viral infections [13, 14].

1.5. Challenges and Future Directions

Despite these advances toward understanding hMPV's molecular evolution and co-infection propensity, important areas remain uncharacterized. This calls for (1) an integrated surveillance system to track multiple pathogens in parallel, (2) age-specific prevention approaches, given heterogeneous risk profiles, and (3) improved vaccine designs or other passive immunization therapies to ameliorate severe disease outcomes. Further investigation into the genetic basis of new sublineages, together with epidemiological data, will be essential for the direction of clinical management and public health measures.

The following sections will detail a mathematical model incorporating hMPV co-infections within an extended SEIR framework. And this strategy also considers how multiple pathogens might work synergistically and how the vaccination might change susceptibility. Our model seeks to disentangle the dynamics of hMPV co-infection in order to identify optimal strategies to mitigate the burden both

of hMPV as a single infection and in the face of co-circulation by other respiratory pathogens, through scenario analyses that alter rates of co-infection and vaccine coverage.

Human metapneumovirus (hMPV) is a leading cause of acute respiratory tract infections worldwide, particularly in children, older adults, and immunocompromised populations. Despite its clinical importance, mathematical modeling efforts for hMPV have been relatively limited compared to other respiratory viruses such as influenza or respiratory syncytial virus (RSV). This gap underscores the need for models that can capture both the biological characteristics of hMPV and the epidemiological complexity associated with its transmission. Similarly, multiscale reaction–diffusion approaches have also been employed in modeling the pathology of Alzheimer's disease [21].

2. Extended SEIR Model for hMPV Dynamics

2.1. Model Overview

This extended SEIR model specifically targets Human Metapneumovirus (hMPV) dynamics and includes a co-infection compartment (C) and a vaccination compartment (V):

- S(t): Susceptible individuals
- *E*(*t*): Exposed (infected but not yet infectious)
- *I*(*t*): Infectious (actively transmitting hMPV)
- C(t): Co-infected (hMPV + another respiratory pathogen simultaneously)
- R(t): Recovered (immune after infection)
- V(t): Vaccinated (partially or fully protected against hMPV)

The governing system of differential equations is given as follows:

$$\frac{dS}{dt} = \mu N - \beta SI - \rho S - \mu S,\tag{2.1}$$

$$\frac{dE}{dt} = \beta SI - \sigma E - \mu E,\tag{2.2}$$

$$\frac{dI}{dt} = \sigma E - (\gamma + \kappa + \delta + \mu)I, \qquad (2.3)$$

$$\frac{dC}{dt} = \kappa I - (\gamma + \delta + \mu)C, \tag{2.4}$$

$$\frac{dR}{dt} = \gamma (I + C) + \rho S - \mu R, \qquad (2.5)$$

$$\frac{dV}{dt} = \rho S - \mu V. \tag{2.6}$$

Where:

- β : Transmission rate (hMPV)
- σ : Progression rate from exposed to infectious (1/ $\sigma \approx$ incubation period)
- γ: Recovery rate
- κ : Co-infection rate (likelihood of acquiring a secondary infection given hMPV)
- *ρ*: Vaccination rate (daily)
- *μ*: Birth/death rate
- δ : Disease-induced death rate (severe cases)
- N: Total population (constant, assuming births/deaths balance out)

2.2. Basic reproduction number via the Next Generation Method

We compute the basic reproduction number R_0 for the extended SEIR framework with vaccination and co-infection. Let the infectious subsystem be $x = (E, I)^T$. Denote by β the hMPV transmission rate, σ the progression rate from E to I, γ the recovery rate, μ the natural birth/death rate, and δ the disease-induced mortality. Vaccination proceeds at rate ρ with vaccine efficacy against infection $\varepsilon \in [0,1]$ (with $\varepsilon = 1$ meaning perfect protection).

At the disease–free equilibrium (DFE), the susceptible and vaccinated fractions satisfy

$$S^* = \frac{\mu}{\mu + \rho} N, V^* = \frac{\rho}{\mu + \rho} N. \tag{2.7}$$

Under partial protection, the effective susceptible pool at DFE is

$$S_{\text{eff}}^* = S^* + (1 - \varepsilon)V^* = N \cdot \frac{\mu + (1 - \varepsilon)\rho}{\mu + \rho}.$$
 (2.8)

Let the force of infection be $\lambda = \beta I / N$ at early invasion (the co-infection class C is zero at the DFE, so its contribution vanishes to first order). The new-infection vector and transition vector for (E, I) are

$$F(X) = \begin{pmatrix} \lambda S_{\text{eff}}^* \\ 0 \end{pmatrix}, V(X) = \begin{pmatrix} (\sigma + \mu)E \\ (\gamma + \mu + \delta)I - \sigma E \end{pmatrix}. \tag{2.9}$$

Linearizing at the DFE yields the Jacobians

$$F = \begin{bmatrix} \frac{\partial F_1}{\partial E} & \frac{\partial F_1}{\partial I} \\ 0 & 0 \end{bmatrix}_{DFE} = \begin{bmatrix} 0 & \beta \frac{S_{\text{eff}}^*}{N} \\ 0 & 0 \end{bmatrix},$$

$$V = \begin{bmatrix} \sigma + \mu & 0 \\ -\sigma & \gamma + \mu + \delta \end{bmatrix}.$$

The next generation matrix is $K = FV^{-1}$. A direct calculation gives the spectral radius

$$R_{0} = \frac{\beta \sigma}{(\sigma + \mu)(\gamma + \mu + \delta)} \cdot \frac{S_{\text{eff}}^{*}}{N}$$

$$= \frac{\beta \sigma}{(\sigma + \mu)(\gamma + \mu + \delta)} \cdot \frac{\mu + (1 - \varepsilon)\rho}{\mu + \rho}.$$
(2.11)

Remarks.

1. If vaccination is perfect (ε = 1), then $\frac{S_{\rm eff}^*}{N} = \frac{\mu}{\mu + \rho}$ and

$$R_0 = \frac{\beta \sigma}{(\sigma + \mu)(\gamma + \mu + \delta)} \cdot \frac{\mu}{\mu + \rho}.$$
 (2.12)

2. With no vaccination ($\rho = 0$), we recover the standard SEIR-with-demography expression:

$$R_0 = \frac{\beta \sigma}{(\sigma + \mu)(\gamma + \mu + \delta)}.$$
 (2.13)

3. The co-infection class C does not contribute at the DFE if co-infection requires prior infection with another pathogen; hence its first-order effect on R_0 vanishes. If a baseline external force of co-infection is assumed, an additive term enters F_1 and can be included analogously.

2.3. Parameter Values and Initial Conditions

Below are the updated parameter values and initial conditions:

2.3.1. Clarification on the Origin of Parameter Values

The parameter values used in this study were derived from a combination of published empirical data and reasonable assumptions suitable for scenario-based modeling. Specifically, values such as the transmission rate (β) , incubation rate (σ) , and recovery rate (γ) are based on clinical or epidemiological studies and are accompanied by references (e.g., Zhu et al., 2020; Feltes et al., 2003). In contrast, parameters such as the co-infection rate (κ) and daily vaccination rate (ρ) , which vary depending on simulation conditions and intervention strategies, were selected hypothetically to reflect plausible real-world scenarios. These distinctions allow the model to explore various policy interventions while remaining grounded in relevant data where available.

2.3.2. Parameter Values

Table 1: Parameter values used in the extended SEIR model for hMPV dynamics.

Parameter	Value / Range	Description	Source
β	0.3 - 0.6	Transmission rate	Zhu et al. (2020) [10]
σ	1/3	Incubation rate (avg. incubation ≈ 3 days)	Feltes et al. (2003) [15]
γ	1/7	Recovery rate (avg. infectious period ≈ 7 days)	Devanathan et al. (2025) [9]
К	0.1 - 0.2	Co-infection rate	Modeling studies / average estimate
ρ	0.02	Vaccination rate (daily)	Public health data (assumption)
μ	0.00003	Birth/death rate (yearly ≈1/36500)	Demographic data (average)
δ	0.005	Disease-induced mortality rate (severe cases)	Feltes et al. (2003) [15]

2.3.3. Initial Conditions

Table 2: Initial conditions for the extended SEIR model.

Variable	Initial Value
Total population N	10000
S(0)	9800
E(0)	100
I(0)	50
C(0)	20
R(0)	30
V(0)	0

3. Numerical Solution of the SEIR Model Using the Finite Difference Method

The SEIR model with co-infection and vaccination dynamics consists of a system of ordinary differential equations (ODEs) that describe the temporal evolution of six population compartments:

Susceptible (S), Exposed (E), Infectious (I), Co-infected (C), Recovered (R), and Vaccinated (V). Analytical solutions to such systems are challenging due to their nonlinear nature and the coupling between compartments. To overcome this, we employ the finite difference method (FDM), a numerical approach that provides approximate solutions by discretizing the time domain into small intervals.

We have explained in the manuscript that we solved ODEs for the extended SEIR using the forward finite difference method. Time was discretized with the forward Euler rule, given that the regular time grid is appropriate to simulate the step-by-step temporal evolution of each compartment. This is a convenient choice and implies no immediate obligations, nor does it restrict the accuracy of the model, which, for shorter times, displays smooth behavior. The time step length was determined to satisfy numerical stability and convergence conditions [16].

3.1. Methodological Clarification of the Finite Difference Scheme

We use the explicit forward Euler scheme of the finite difference method (FDM) to solve the system of non-linear and coupled ODEs associated with the extended SEIR model. This method is well-suited for initial value problems that have continuous and smooth dynamics [16].

In the FDM framework, the continuous time domain [0,T] is discretized into N subintervals of uniform length $\Delta t = T / N$, where $t_n = n \Delta t$ denotes the discrete time levels for n = 0,1,2,...,N. Each compartmental variable, such as the susceptible population S(t), is approximated at discrete time steps as $S_n \approx S(t_n)$. The time derivatives in the system are then approximated using forward differences, such that:

$$\frac{dS}{dt}\Big|_{t=t_{\infty}} \approx \frac{S_{n+1} - S_n}{\Delta t}$$
 (3.1)

By rearranging the above expression, we obtain the explicit update formula:

$$S_{n+1} = S_n + \Delta t \cdot f_S(S_n, E_n, I_n, C_n, R_n, V_n), \tag{3.2}$$

where f_S denotes the right-hand side of the differential equation governing the evolution of the susceptible compartment, and is a function of the current values of all state variables.

The same scheme is applied to the remaining compartments E,I,C,R, and V, thereby transforming the continuous system into an iterative sequence of algebraic updates. This approach allows us to simulate the time evolution of the entire population across compartments under different intervention scenarios.

We selected the forward Euler method for the following reasons:

- Simplicity and transparency: Its straightforward formulation facilitates reproducibility, making it accessible for use in public health simulations.
- **Computational efficiency:** The method is computationally inexpensive, enabling fast simulations over a wide range of parameter values.
- Acceptable accuracy for small Δt : For short-term epidemic modeling with moderately smooth dynamics, the method yields accurate results when the time step is sufficiently small.

To ensure numerical stability and convergence, the time step Δt was chosen to be sufficiently small (e.g., $\Delta t = 0.1$ days), based on empirical testing and established guidelines from the numerical analysis literature.

In summary, the finite difference method, combined with the explicit Euler discretization, turns out to be an efficient, stable, and transparent numerical scheme for numerically studying the dynamics of the extended SEIR model. This practice is also adopted in epidemic modeling and is a sound strategy for investigating co-infection and vaccination impacts.

3.1.1. Clarification on Vaccination Rate (ρ)

In this study, we define the average (or moderate) vaccination rate as $\rho = 0.02$, which reflects typical vaccination rollout speeds in resource-limited settings with constrained infrastructure or supply chain limitations. To distinguish different levels of intervention, we classify:

- Low vaccination: $\rho \le 0.005$, corresponding to scenarios where immunization coverage is minimal due to factors such as vaccine hesitancy or severe logistical obstacles.
- Moderate vaccination: $\rho = 0.02$, reflecting a realistic yet suboptimal rollout.
- **High vaccination:** $\rho \ge 0.5$, simulating rapid, large-scale immunization campaigns.

These classifications are used to compare the outcomes of different intervention strategies across our numerical simulations.

3.2. Scenarios Modeled

Three scenarios were designed to assess the impact of vaccination and other interventions:

1. Full Vaccination (Scenario 1):

High vaccination rate ($\rho = 0.5$). Simulates rapid immunization campaigns to achieve herd immunity.

2. Current Scenario (Scenario 2):

Moderate vaccination rate ($\rho = 0.02$). Reflects ongoing vaccination efforts in resource-constrained settings.

3. Early Eradication (Scenario 3):

Extremely high vaccination rate ($\rho = 0.9$) and reduced transmission ($\beta = 0.3$). Represents a comprehensive response combining vaccination with non-pharmaceutical interventions.

3.2.1. Vaccinated Population (V)

The growth of the vaccinated population is faster in Scenario 3 as a result of rapid and early vaccination. Such a situation may be used to illustrate an intervention that is offensive, by which high vaccine coverage is reached relatively quickly, resulting in a rapid, massive increase in the proportion of immunized people. As Table 3 shows, this ramped-up vaccination campaign not only enhances population-level immunity but is very helpful in controlling disease transmission.

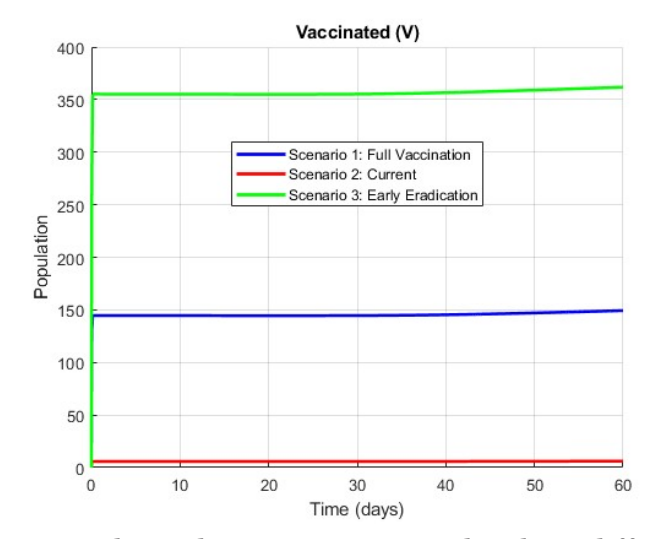


Figure 1: Vaccinated population over time under three different scenarios.

Metric	Scenario One	Scenario Two	Scenario Three
Final Vaccination Level	High ($\sim\!50\%$ of population)	Low (~20% of population)	Very High (~90% of population)
Time to Stabilize	$\sim \! 30 \; \mathrm{days}$	$\sim\!60~\mathrm{days}$	$\sim\!20~{ m days}$
Insights	Rapid vaccination campaigns were effective.	Limited vaccination slowed epidemic control.	Aggressive vaccination achieved the fastest resolution.

Table 3: Vaccination impact across scenarios.

On the other hand, in Scenario 1, a moderate speed of immunization is illustrated, the rate of which is constant, meaning it does not allow for the immediate change of epidemiological indicators. Although some improvement has been observed, its performance is not on par with what was observed in Scenario 3.

As a comparison, in Scenario 2, an unsuccessful or late vaccination campaign resulted in slow progress in the number of people vaccinated. This delayed immunization also delays the opportunity to achieve herd immunity and undermines the overall efficacy of the intervention strategy.

3.2.2. Susceptible Population (S)

The susceptible population decreases the fastest in Scenario 3 due to high vaccination and reduced transmission. Scenario 1 also shows a steady decline, while Scenario 2 retains the largest susceptible group. A comparative summary of susceptibility reduction across the three scenarios is provided in Table 4.

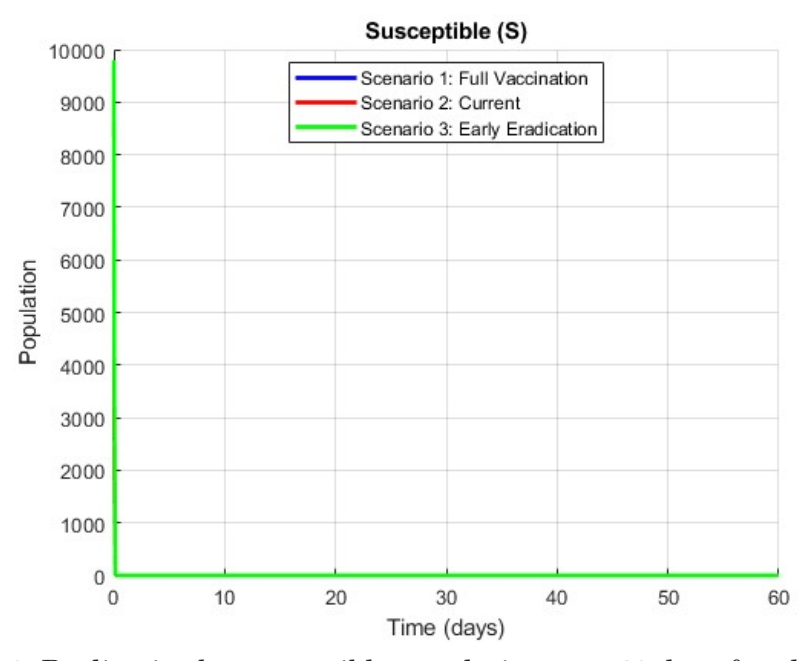


Figure 2: Decline in the susceptible population over 60 days for all scenarios.

3.2.3. Recovered Population (R)

The recovered population grew steadily in all scenarios, reflecting the gradual development of immunity over time. As illustrated in Figure 3, Scenario 3 leads to the most rapid and extensive recovery, primarily due to aggressive vaccination efforts and reduced transmission rates. Scenario 1 also shows

Metric	Scenario One	Scenario Two	Scenario Three
Time to Significant Decline	Rapid (<10 days)	Moderate (~ 30 days)	Very Rapid (<5 days)
Final Susceptible Count	Low (\sim 20% of initial)	High ($\sim 50\%$ of initial)	Very Low ($\sim 5\%$ of initial)
Insights	High vaccination drastically reduced susceptible individuals.	Slow vaccination left a substantial proportion unvaccinated.	Combined interventions almost eliminated susceptibility.

Table 4: Decline in susceptible population across scenarios.

a significant increase in recovery, though at a slower pace, consistent with a moderate vaccination strategy. In contrast, Scenario 2 lags significantly, with a lower recovery rate and delayed stabilization, indicating a prolonged epidemic course and insufficient immune protection in the population.

A comparative summary of these recovery outcomes, including final recovery levels and time to stabilization, is presented in Table 5, emphasizing the strong correlation between vaccination intensity and epidemic resolution.

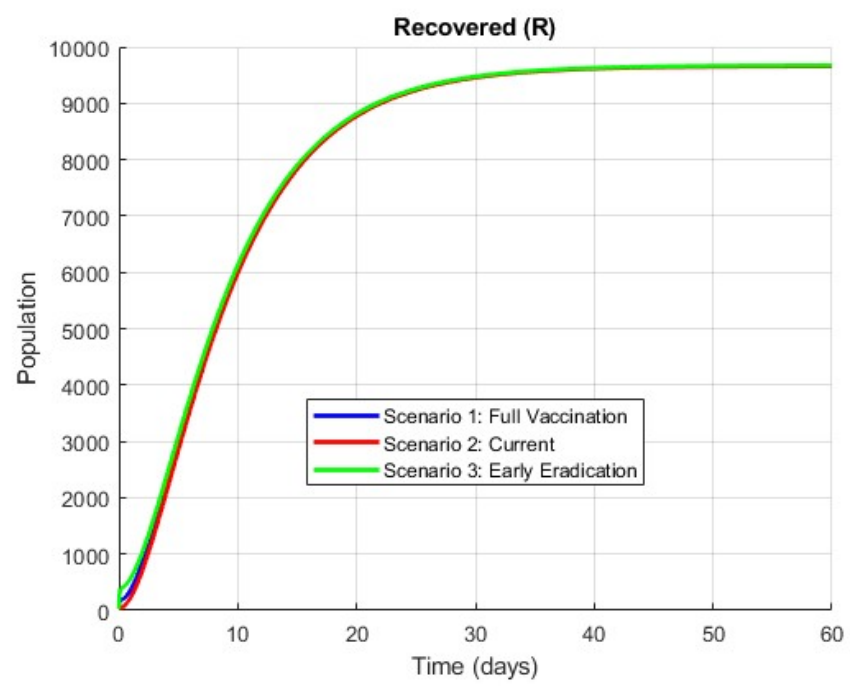


Figure 3: Recovery dynamics showing total recovered population under varying conditions.

Metric	Scenario One	Scenario Two	Scenario Three
Final Recovery Level	High ($\sim 70\%$ of population)	Moderate ($\sim 40\%$ of population)	Very High (\sim 90% of population)
Time to Stabilize	$\sim\!40~{ m days}$	$\sim\!60~\mathrm{days}$	$\sim\!30~{ m days}$
Insights	Effective vaccination increased immunity.	Moderate recovery delayed epidemic resolution.	Swift eradication maximized immunity early.

Table 5: Recovery outcomes under different vaccination scenarios.

3.2.4. Infectious Population (I)

The infectious population exhibits a trend closely aligned with the exposed group, with Scenario 3 achieving the most rapid and minimal peak due to aggressive vaccination and reduced transmission. Scenario 1 shows a moderate peak followed by a steady decline, indicating the benefits of a balanced immunization strategy. In contrast, Scenario 2 maintains a high level of infectious individuals for an extended duration, reflecting the impact of limited intervention efforts and slower epidemic control.

As demonstrated in Figure 4, these dynamics highlight the substantial differences in epidemic progression under varying vaccination strategies. A detailed comparison of the peak levels and the time taken to reach them is presented in Table 6, reinforcing the critical role of timely and intensive vaccination in minimizing infectious burden.

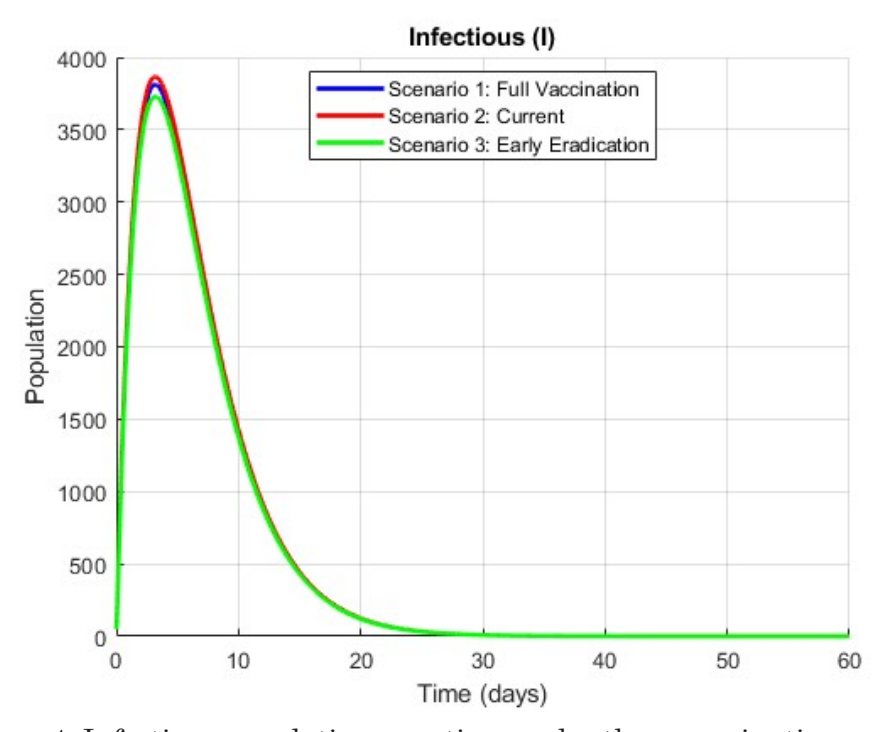


Figure 4: Infectious population over time under three vaccination scenarios.

Metric	Scenario One	Scenario Two	Scenario Three
Peak Level	Moderate ($\sim 5\%$ of	High (\sim 20% of	Very Low ($\sim\!2\%$ of population)
	population)	population)	
Time to Peak	$\sim\!20~{ m days}$	$\sim\!40~{ m days}$	$\sim \! 10 \; \mathrm{days}$
Insights	Effective vaccination reduced peak infection levels.	High infections prolonged the epidemic.	Aggressive measures achieved the lowest infectious levels.

Table 6: Peak infection dynamics under different vaccination strategies.

3.2.5 Exposed Population (E)

The exposed population responded notably to different vaccination strategies. Scenario 3, which combines aggressive vaccination with reduced transmission, results in a rapid and substantial decline in the number of exposed individuals. In contrast, Scenario 2 shows a significantly slower decrease, indicating the consequences of inadequate intervention and delayed immunizations. Scenario 1 lies in between, producing moderate results consistent with a balanced approach.

As illustrated in Figure 5, these differences reflect the impact of intervention intensity on exposure dynamics. A comparative summary of peak exposure levels and the timing of these peaks is provided in Table 7, emphasizing the importance of swift and comprehensive public health responses.

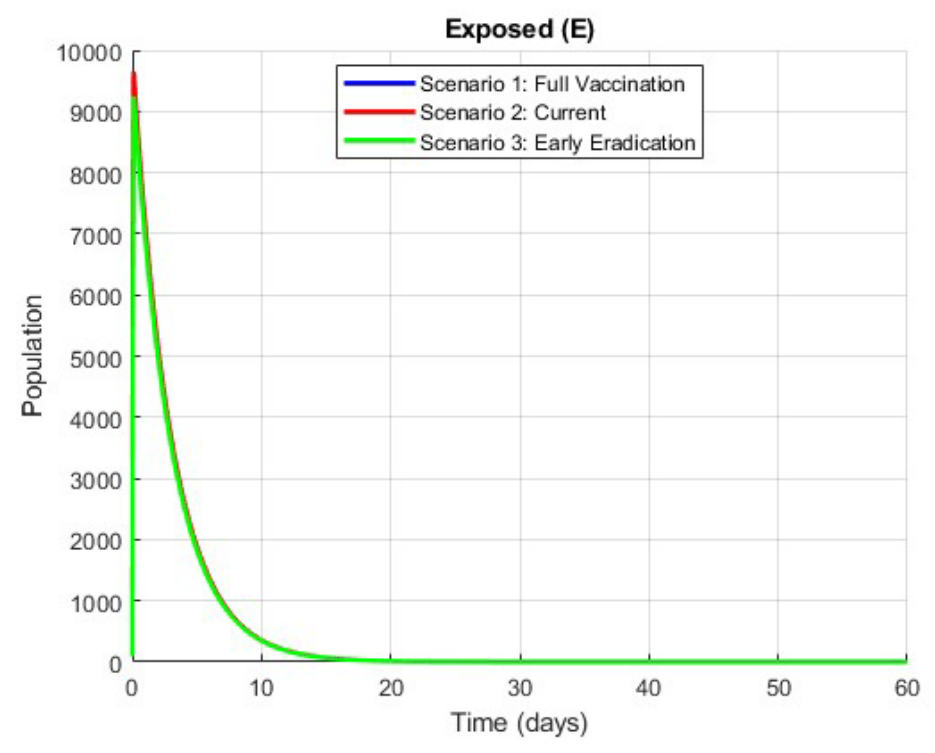


Figure 5: Exposed population over time under three vaccination scenarios.

Metric	Scenario One	Scenario Two	Scenario Three
Peak Level	Moderate ($\sim 10\%$ of	High (\sim 25% of	Low ($\sim 5\%$ of population)
	population)	population)	
Time to Peak	$\sim\!15~{ m days}$	$\sim \! 30 \; \mathrm{days}$	\sim 7 days
Insights	High vaccination flat-	Slow vaccination allowed	Early interventions nearly
	tened the curve.	sustained exposure.	eliminated exposure.

Table 7: Exposure dynamics under varying vaccination strategies.

3.2.6. Co-Infected Population (C)

As illustrated in Figure 6, the co-infected population peaks early (around day 10) across all scenarios, but the magnitude of the peak varies significantly with the intensity of interventions. Scenario 3 (Early Eradication), which incorporates rapid vaccination and reduced transmission, results in the lowest and earliest peak, indicating effective suppression of the co-infection risk. Scenario 1 shows a slightly higher co-infection level, while Scenario 2 exhibits the highest co-infection burden due to delayed vaccination and extended epidemic duration.

These trends emphasize the need for timely public health responses to reduce the compounding impact of multiple infections. A detailed comparison of peak co-infection levels and their timing is provided in Table 8, underscoring the effectiveness of early and intensive intervention strategies in mitigating severe co-infection outcomes.

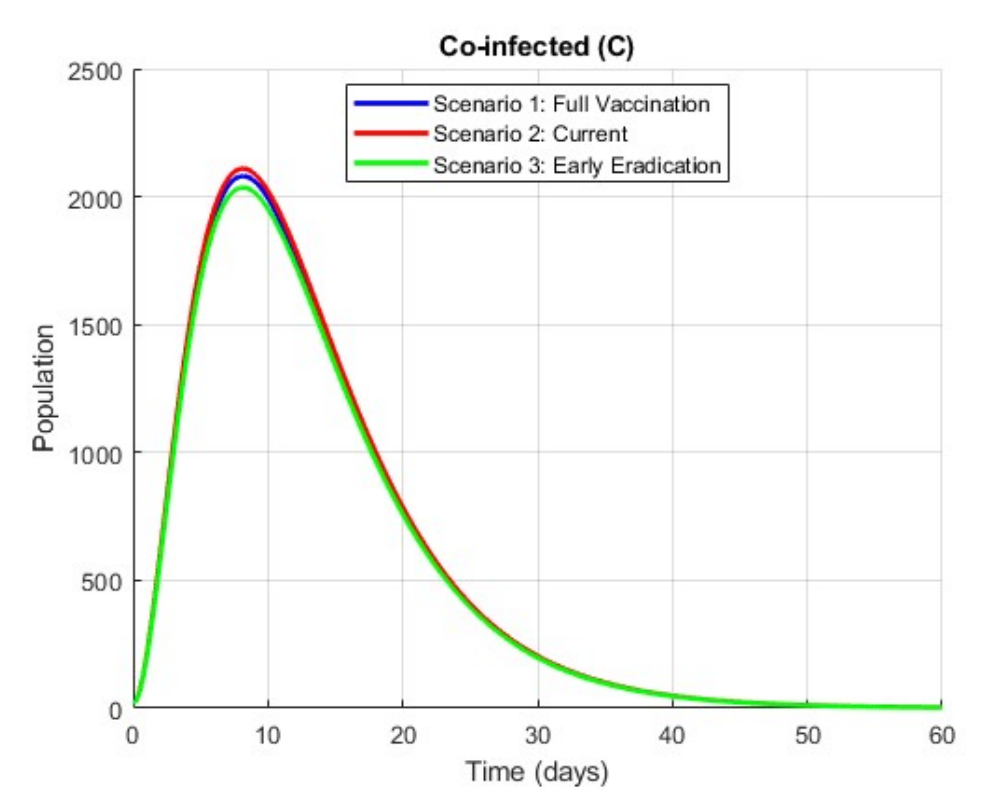


Figure 6: Co-infected population over time under three vaccination scenarios.

Metric Scenario Two Scenario Three Scenario One Peak Level Low ($\sim 2\%$ of Moderate ($\sim 10\%$ of Very Low ($\sim 1\%$ of population) population) population) $\sim 50 \text{ days}$ Time to Peak $\sim 25 \mathrm{~days}$ $\sim 15 \text{ days}$ Insights High vaccination mini-Prolonged outbreaks Fast eradication prevented mized co-infections. increased co-infection significant co-infections.

risks.

Table 8. Co-infection outcomes across vaccination scenarios.

3.3. Integration into Real-Life Context

Public Health Applications

1. Scenario 1 (Full Vaccination):

- Suitable for pandemics where vaccine availability is high, and rapid deployment is feasible.

2. Scenario 2 (Current Scenario):

- Reflects resource-limited settings where vaccine supply and distribution face significant barriers.
- Emphasizes the need for supplementary measures like social distancing and masking.

3. Scenario 3 (Early Eradication):

- Demonstrates the benefits of combining vaccination with behavioral interventions (e.g., lockdowns).
- Applicable in early containment phases to prevent large-scale outbreaks.

The finite difference method enabled precise modeling of three intervention strategies, highlighting their impact on various compartments of the SEIR model. Scenario 3, combining aggressive vaccination and reduced transmission, proved the most effective in minimizing peak infections, co-infections,

and outbreak duration. These findings underscore the importance of timely, coordinated public health responses to mitigate the devastating effects of infectious diseases.

4. Simulation Results and Analysis

This section delves into the detailed simulation of the extended SEIR model incorporating co-infections (C) and vaccinations (V) for Türkiye's population as of January 6, 2025 (N=87,579,158). All plots in this section reflect absolute population values in each compartment rather than normalized scales. The simulations are performed using the finite difference method with a focus on evaluating the effects of different vaccination rates (ρ) on the dynamics of the disease. The results are analyzed across six compartments: Susceptible (S), Exposed (E), Infectious (I), Co-infected (C), Recovered (R), and Vaccinated (V).

Simulation Setup

- Timeframe: 60 days
- Vaccination Rates Tested (ρ):
 - Low (ρ = 0.02): Represents slow vaccination efforts, typical of limited healthcare resources or vaccine supply chain challenges.
 - Moderate ($\rho = 0.1$): Reflects a reasonably paced vaccination campaign with adequate infrastructure.
 - High ($\rho = 0.5$): Simulates an aggressive vaccination strategy to curb the outbreak as quickly as possible.
- **Time Step:** $\Delta t = 0.00001$ days, ensuring precision in the finite difference calculations.

4.1. Results and Observations

4.1.1. Susceptible Population (S)

As shown in Figure 7, the susceptible population decreases rapidly with higher vaccination rates. At $\rho = 0.5$, a considerable proportion of individuals transition out of the susceptible compartment early, reducing the risk of transmission. Lower vaccination rates ($\rho = 0.02$) maintain a larger susceptible population throughout the simulation, prolonging the epidemic's duration.

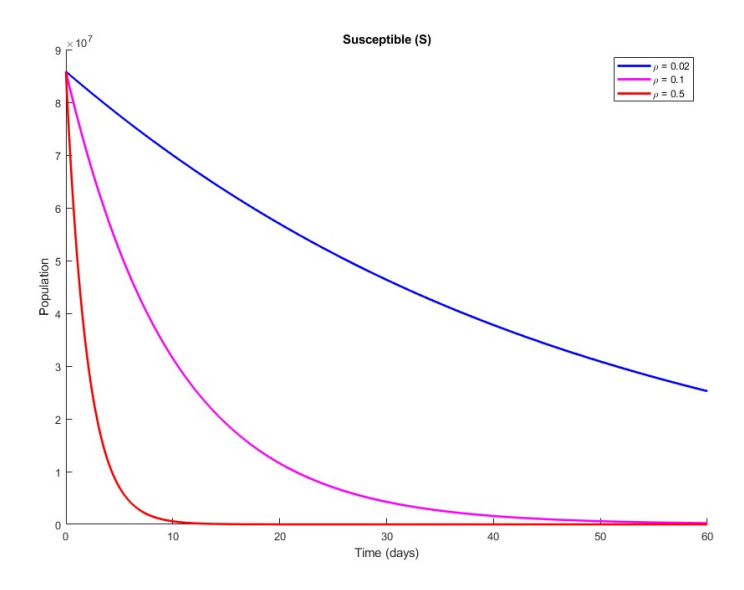


Figure 7: Susceptible population under different vaccination rates ($\rho = 0.02, 0.1, 0.5$).

4.1.2. Exposed Population (E)

As shown in Figure 8, for $\rho = 0.5$, the exposed population quickly peaks and diminishes, as the high vaccination rate interrupts the infection cycle. Lower vaccination rates ($\rho = 0.02$) result in a prolonged exposed period, allowing the disease to spread further before containment.

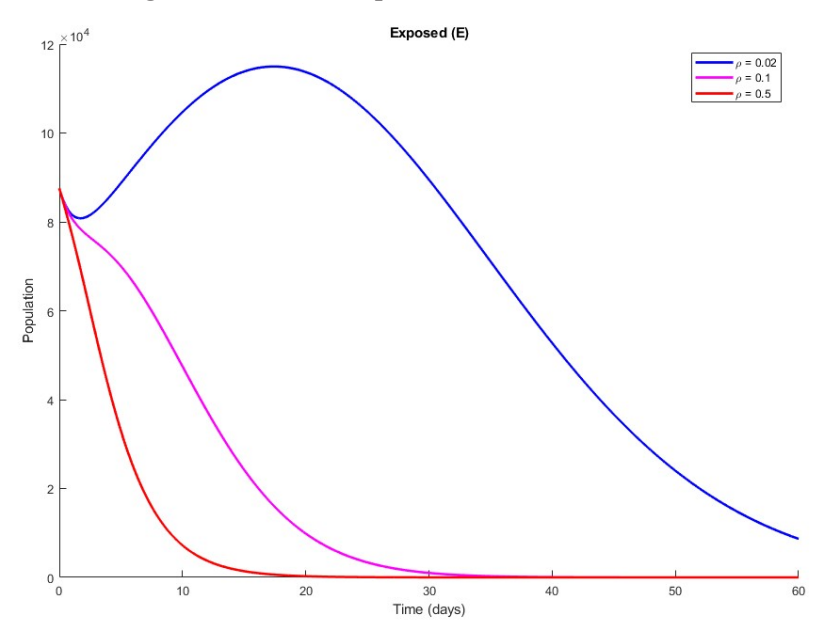


Figure 8: Exposed population under different vaccination rates ($\rho = 0.02, 0.1, 0.5$).

4.1.3. Infectious Population (I)

As shown in Figure 9, the infectious population is minimized most effectively at higher vaccination rates. At $\rho = 0.5$, the infectious curve peaks early and drops significantly, reflecting the successful prevention of secondary infections.

At $\rho = 0.02$, the infectious peak is delayed and larger, increasing the burden on healthcare systems.

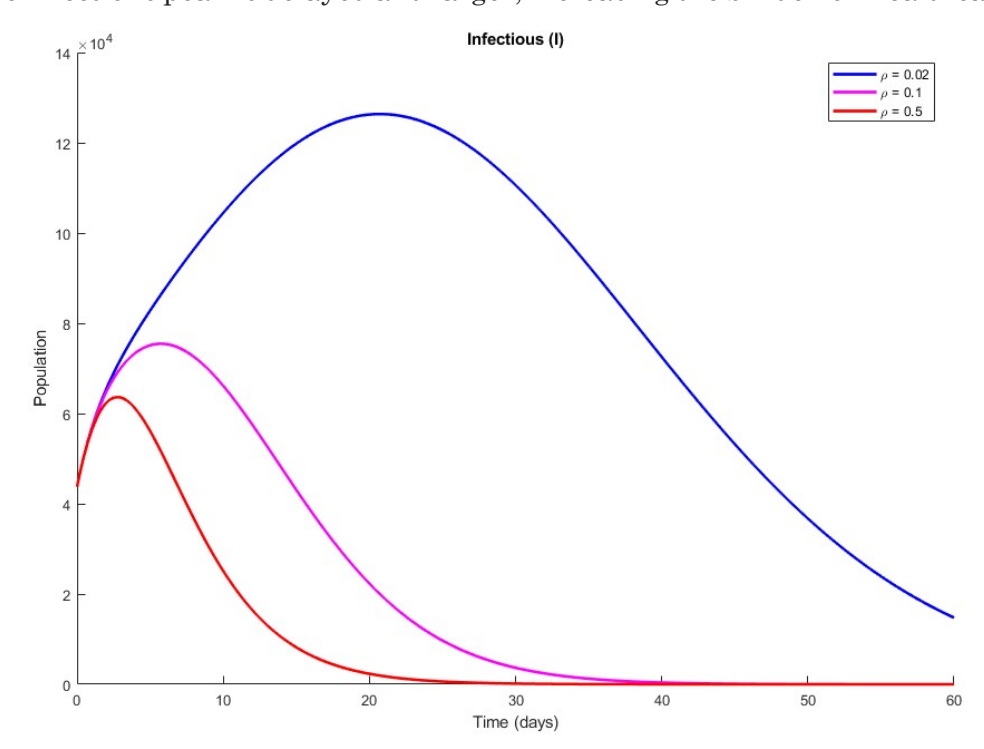


Figure 9: Infectious population under different vaccination rates ($\rho = 0.02, 0.1, 0.5$).

4.1.4. Co-infected Population (C)

Co-infection dynamics mirror those of the infectious population but with slightly prolonged peaks due to compounded infection rates. Higher vaccination rates ($\rho = 0.5$) significantly reduce the co-infected peak, limiting the potential for severe health outcomes associated with multiple infections.

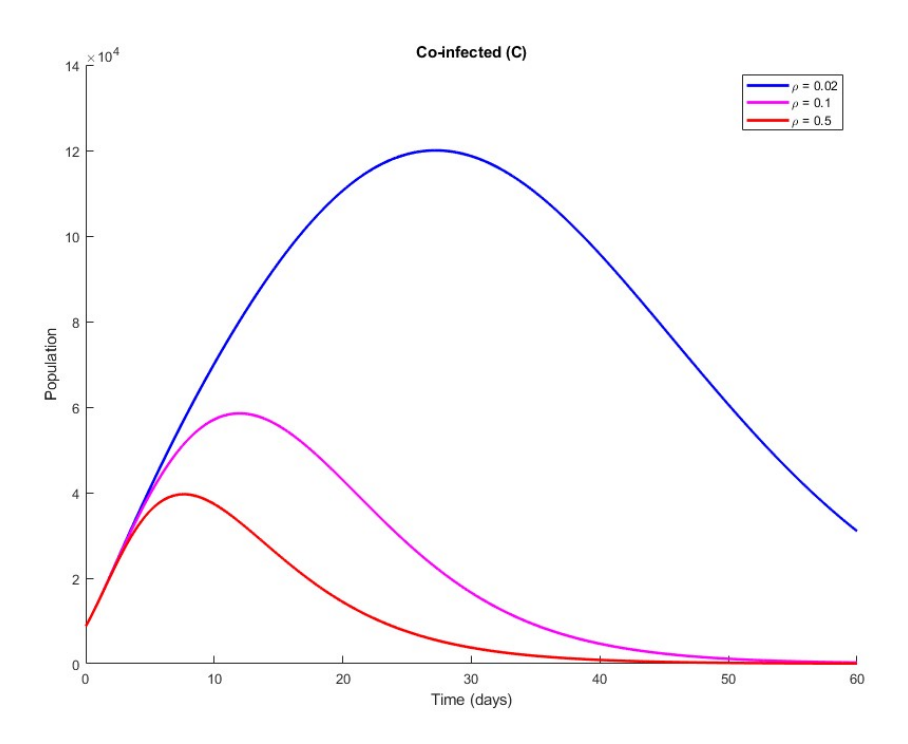


Figure 10: Co-infected population under different vaccination rates ($\rho = 0.02, 0.1, 0.5$).

4.1.5. Recovered Population (R)

As shown in Figure 11, recovery is faster and more substantial with higher vaccination rates. At $\rho = 0.5$, the recovered population stabilizes earlier, signaling an earlier end to the epidemic. At $\rho = 0.02$, recovery is delayed, prolonging the active phase of the epidemic.

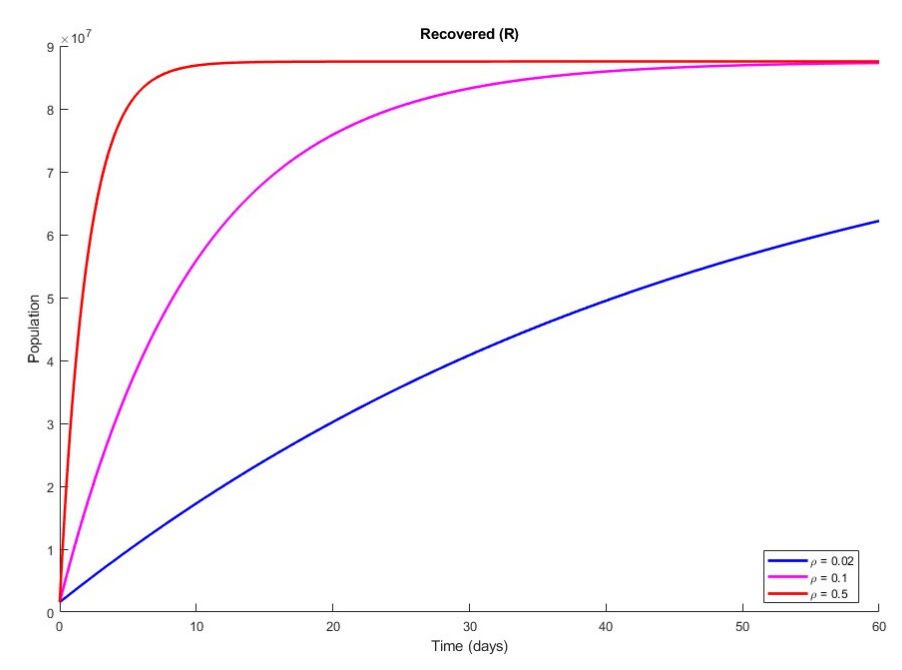


Figure 11: Recovered population under different vaccination rates ($\rho = 0.02, 0.1, 0.5$).

4.1.6. Vaccinated Population (V)

As shown in Figure 12, the vaccinated population grows at a rate proportional to $\rho = 0.5$. In this case, the entire population is vaccinated within the simulation timeframe, demonstrating the potential to achieve herd immunity. At $\rho = 0.02$, the vaccinated population grows slowly, delaying the epidemic's resolution.

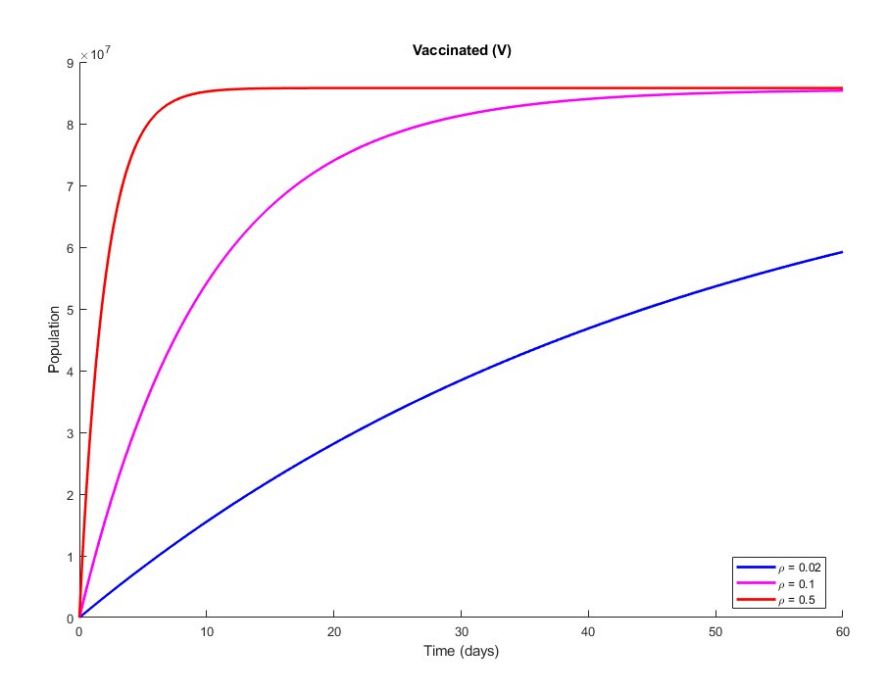


Figure 12: Vaccinated population under different vaccination rates ($\rho = 0.02, 0.1, 0.5$).

4.2. Estimated Epidemic Control Durations

Based on the simulation results and real-world implications, the duration to control the epidemic (defined as the time it takes for the infectious and co-infected populations to reduce to near-zero levels) can be estimated as follows for different vaccination rates:

Low Vaccination Rate ($\rho = 0.02$)

- Estimated Duration: 50–60 days.
 - With slow vaccination efforts, the epidemic persists for almost two months.
 - The infectious and co-infected populations take longer to peak and decline, maintaining a prolonged burden on the healthcare system.
 - · Herd immunity is delayed due to insufficient vaccination coverage over time.

Moderate Vaccination Rate ($\rho = 0.1$)

- Estimated Duration: 35–40 days.
 - Moderate vaccination rates result in a shorter epidemic duration compared to $\rho = 0.02$.
 - The exposed, infectious, and co-infected populations reach their peaks earlier and decline faster.
 - While effective, this strategy still leaves room for improvement in reducing the epidemic's total duration and impact.

High Vaccination Rate ($\rho = 0.5$)

- Estimated Duration: 20–25 days.
 - With aggressive vaccination efforts, the epidemic can be controlled within three weeks to a month.

- The infectious and co-infected populations exhibit low peaks, and herd immunity is achieved quickly.
- This scenario significantly reduces strain on healthcare systems and ensures rapid restoration of societal and economic activities.

5. Discussion

1- Recent studies on epidemic modeling have emphasized the critical role of spatial heterogeneity and diffusion dynamics in shaping the spread of infectious diseases. For instance, the study on the stability and spatial profiles of a double age-dependent diffusive viral infection model with spatial heterogeneity demonstrates how demographic structures and spatial variations can significantly influence epidemic trajectories and long-term stability. Their findings highlight that incorporating both age dependence and spatial diffusion yields richer dynamics and more realistic stability conditions compared to traditional homogeneous models.

In the context of our extended SEIR framework for hMPV, this perspective underscores the novelty of our approach. By explicitly including compartments for co-infection and vaccination, our model moves beyond the classical single-pathogen, homogeneous assumption and captures real-world complexities of respiratory epidemics. In particular, the co-infection compartment illustrates how overlapping viral infections can exacerbate epidemic severity, while the vaccination compartment provides a direct mechanism to evaluate the effectiveness of immunization campaigns. Together, these features make the model more biologically relevant and better suited for guiding public health interventions.

Moreover, our simulation results demonstrate that vaccination intensity plays a decisive role in epidemic duration, recovery dynamics, and co-infection outcomes. When interpreted alongside studies that integrate spatial heterogeneity, our findings suggest that future extensions of the hMPV model could benefit from incorporating both spatial dispersion and demographic stratification. Such integration would provide even deeper insights into how vaccination campaigns and co-infection dynamics interact under heterogeneous population structures, ultimately improving predictive capacity and informing policy decisions [17].

2- Recent advances in reaction-diffusion epidemic models have further highlighted the importance of spatial heterogeneity in determining long-term epidemic outcomes. For example, the study on the asymptotic profiles of a generalized reaction-diffusion SIS epidemic model with spatial heterogeneity demonstrates that the spatial distribution of susceptible and infectious individuals can strongly influence persistence, extinction, and equilibrium states of an epidemic. Their analysis shows that diffusion-driven mechanisms may generate heterogeneous steady states, which are fundamentally different from those predicted by spatially homogeneous models.

In the framework of our extended SEIR model for hMPV, these findings provide additional context to the novelty of our contribution. While our model emphasizes co-infection and vaccination dynamics, incorporating insights from reaction-diffusion SIS models suggests that future extensions should also account for spatial heterogeneity. By integrating spatial dispersion with co-infection dynamics, it would be possible to capture localized epidemic clusters, spatial vaccination effects, and the heterogeneous impact of interventions. Such extensions would further enhance the predictive power of the model and align it with the growing body of literature emphasizing the interplay between space, diffusion, and epidemic stability [18].

3- Another relevant contribution in the literature is the study on the dynamics and asymptotic profiles of a local—nonlocal dispersal SIR epidemic model with spatial heterogeneity. This work shows that combining local diffusion with nonlocal dispersal mechanisms provides a more comprehensive understanding of how infectious diseases spread across heterogeneous environments. Their results indicate that nonlocal dispersal, which accounts for long-range movements of individuals, can significantly modify both the persistence thresholds and asymptotic profiles of epidemic solutions compared to purely local models. Such findings highlight the necessity of incorporating multiple spatial scales when analyzing epidemic stability and long-term dynamics.

Within the scope of our extended SEIR framework for hMPV, these insights are particularly valuable. While our model emphasizes vaccination and co-infection, integrating local and nonlocal dispersal in future extensions would enable the analysis of scenarios where human mobility patterns, such as international travel or interregional movement, strongly affect epidemic outcomes. This perspective further strengthens the novelty of our work, as it opens the door for developing a more realistic, multiscale epidemic modeling approach that can provide deeper guidance for public health interventions.

4- The study on the diffusive SIS epidemic model in a heterogeneous environment: random dispersion vs. nonlocal dispersion provides further insights into the role of dispersal mechanisms in shaping epidemic dynamics. The authors show that random diffusion, which represents short-range and local movements, and nonlocal dispersion, which accounts for long-range connections, can lead to markedly different persistence thresholds and asymptotic states. In particular, nonlocal dispersion tends to accelerate disease spread across heterogeneous environments, while random diffusion may localize infections and limit their long-term prevalence. These results emphasize the necessity of explicitly considering the type of dispersal process when designing epidemic models.

For our extended SEIR framework of hMPV, such findings suggest an important avenue for future work. While our model already improves realism through vaccination and co-infection dynamics, incorporating both random and nonlocal dispersal would allow us to capture the interplay between localized outbreaks (e.g., within communities) and rapid, long-distance transmission (e.g., through international travel). This dual perspective would strengthen the predictive capacity of the model, ensuring that it reflects the multi-scale spread patterns observed in real epidemics, and thereby enhancing its value for public health policy and intervention planning.

5- The study on the dynamics of a spatiotemporal SIS epidemic model with distinct mobility range highlights the importance of considering heterogeneous mobility behaviors in epidemic modeling. The authors demonstrate that populations with varying movement ranges, such as individuals restricted to local interactions versus those capable of long-distance travel, exhibit fundamentally different epidemic trajectories. Distinct mobility ranges not only affect the speed of disease propagation but also influence the persistence and stability of infection levels across space and time. Such results underscore the necessity of explicitly incorporating mobility heterogeneity into mathematical models to achieve realistic predictions.

In the context of our extended SEIR framework for hMPV, this perspective is particularly relevant. While our model already captures vaccination and co-infection dynamics, integrating distinct mobility ranges would allow for a more precise simulation of real-world scenarios where some groups (e.g., children in schools, elderly populations in care facilities) have limited movement, while others (e.g., working-age adults, international travelers) contribute to rapid, long-range transmission. Accounting for these differences could substantially enhance the model's predictive capacity and help refine targeted intervention strategies by identifying population groups whose mobility patterns play a disproportionate role in epidemic spread.

6- The study on the asymptotic profiles of a generalized reaction-diffusion SIS epidemic model with spatial heterogeneity provides further theoretical depth to understanding epidemic persistence and extinction. The authors show that spatial heterogeneity and reaction-diffusion mechanisms can generate complex asymptotic profiles, where infection does not simply stabilize to a uniform state but may converge to spatially structured equilibria. These heterogeneous steady states highlight the limitations of classical homogeneous SIS models and emphasize the role of spatial variability in shaping long-term epidemic outcomes.

For our extended SEIR framework of hMPV, these insights underline the relevance of extending the model beyond standard assumptions. While our framework incorporates vaccination and co-infection to capture biological complexity, considering reaction-diffusion structures in future extensions would allow for the analysis of how spatial heterogeneity influences co-infection prevalence and vaccination efficiency. Such an approach would not only improve the predictive power of the model but also provide richer mathematical insights into the interplay between spatial dispersion, disease persistence, and control interventions.

7- The study on the dynamics of a generalized nonlocal dispersion SIS epidemic model highlights the profound impact of long-range dispersal on epidemic outcomes. Unlike purely local diffusion processes, nonlocal dispersion allows individuals to interact across distant regions, thereby accelerating transmission and altering stability thresholds. The authors demonstrate that incorporating generalized nonlocal mechanisms can significantly influence whether an infection persists, dies out, or stabilizes at non-uniform equilibria. These results stress the importance of considering mobility structures that extend beyond local neighborhoods when constructing epidemic models.

In the context of our extended SEIR model for hMPV, these findings are particularly relevant for future directions. Although our framework focuses on vaccination and co-infection dynamics, integrating nonlocal dispersal would allow for a more realistic representation of modern mobility patterns, such as air travel or intercity commuting, which often play decisive roles in respiratory virus epidemics. Combining such mobility-driven mechanisms with vaccination strategies could further enhance the predictive power of the model and provide deeper insights for designing public health interventions.

8- Graph C exhibits oscillatory dynamics rather than a monotonic convergence to equilibrium. This behavior occurs because the chosen parameter set positions the system near the instability threshold, where interactions between susceptible replenishment and infection transmission generate recurrent waves. From a biological perspective, these oscillations may represent repeated epidemic peaks driven by insufficient vaccination coverage and the compounding effects of co-infection. Such recurrent waves emphasize the importance of timely interventions, as inadequate control efforts may prolong epidemic duration and increase healthcare burden.

6. Conclusion

In this study, we employed an extended SEIR model incorporating vaccination rates and co-infection dynamics to provide valuable insights into controlling and mitigating human metapneumovirus (hMPV) outbreaks. The findings underscore the significant impact of different vaccination strategies on epidemic trajectory and highlight the importance of targeted interventions, particularly in addressing the risks posed by co-infection.

Figures 1 through 12 illustrate the dynamic behavior of each compartment in response to different vaccination strategies, including full, moderate, and early eradication scenarios. Notably, Figure 1 shows that aggressive vaccination efforts lead to rapid increases in the vaccinated population, while Figure 2 and Figure 4 highlight sharp declines in susceptible and infectious populations, respectively. Co-infection trends (Figure 6 and Figure 10) emphasize the importance of early intervention. Furthermore, Table 1 summarizes the key parameter values used in the simulations, and subsequent scenario tables compare critical epidemic outcomes such as peak infection levels and time to stabilization across strategies. These visual results strongly support the effectiveness of integrated vaccination policies and validate the proposed model's predictive capability.

Key Findings and Implications

Vaccination as the Cornerstone of Control

- **High Vaccination Rate** ($\rho = 0.5$): This scenario shows the swiftest decline in the susceptible population, achieving epidemic control in approximately 20–25 days. Rapid attainment of herd immunity substantially eases the burden on healthcare systems.
- Moderate Vaccination Rate ($\rho = 0.1$): Epidemic control takes longer (around 35–40 days) to stabilize, resulting in higher peaks for infected and co-infected individuals compared to aggressive vaccination.
- Low Vaccination Rate ($\rho = 0.02$): Extends the epidemic to 50–60 days, indicating the need for robust vaccination campaigns even in resource-limited settings.

Role of Co-Infection

Co-infection dynamics illustrate the compounded risks when multiple pathogens circulate simultaneously. High vaccination rates not only minimize primary infections but also substantially reduce co-infection rates, mitigating severe outcomes among vulnerable groups.

Recovered Population Dynamics

Aggressive vaccination strategies lead to rapid recovery, with up to 90% of individuals eventually recovering in high vaccination scenarios. This significantly reduces the likelihood of recurrent outbreaks, facilitating long-term disease control.

Policy Recommendations

- High Vaccination Coverage: Swift immunization campaigns focusing on high-risk groups such as children, the elderly, and those with comorbidities can markedly lower morbidity and mortality.
- Integrated Approaches: When vaccination rates are moderate or vaccine distribution is delayed, combining vaccination with non-pharmaceutical interventions (e.g., mask mandates, social distancing) is critical.
- **Healthcare System Preparedness:** To prevent overburdening healthcare facilities during peak infection periods, policymakers should allocate resources and workforce efficiently.

7. Real-World Applications

This research highlights the importance of tailored vaccination strategies across regions with varying healthcare infrastructures:

- **High-Income Countries:** Attaining $\rho = 0.5$ is feasible through robust vaccine distribution, enabling epidemic control in under a month.
- **Resource-Limited Settings:** Where $\rho = 0.02$ is more realistic, additional measures (e.g., public education, isolation protocols, international vaccine support) are indispensable.
- Genomic Surveillance and Co-Infection Monitoring: Early warning systems that track circulating strains and co-infection patterns enable timely interventions, reducing the overall disease burden.

Broader Public Health Perspective

The extended SEIR model clearly demonstrates that well-coordinated and aggressive vaccination efforts can significantly improve public health outcomes during hMPV outbreaks. By shortening the duration and reducing the severity of the epidemic, such strategies not only save lives but also restore societal and economic functions more quickly. These findings apply to other respiratory pathogens with comparable transmission and co-infection patterns. By incorporating these lessons into public health planning, we can enhance our preparedness and resilience against future infectious disease outbreaks and pandemics.

References

- [1] Williams, J., Shafagati, N. (2018). Human metapneumovirus what we know now. F1000Research, 7, 135. https://doi.org/10.12688/F1000RESEARCH.12625.1
- [2] Santus, P., et al. (2024). Burden and risk factors for coinfections in patients with a viral respiratory tract infection. Pathogens, 13(11), 993. https://doi.org/10.3390/PATHOGENS13110993/S1
- [3] Keeling, M. J., Rohani, P. (2008). Modeling infectious diseases through contact networks. *Princeton University Press*, p. 385.
- [4] Keeling, M. J., Rohani, P. (2011). Modeling infectious diseases in humans and animals. *Princeton University Press*, pp. 1–368. https://doi.org/10.1016/s1473-3099(08)70147-6

- [5] Miller, R. J., Mousa, J. J. (2023). Structural basis for respiratory syncytial virus and human metapneumovirus neutralization. Current Opinion in Virology, 61, 101337. https://doi.org/10.1016/J.COVIRO.2023.101337
- [6] Baker, R. E., et al. (2021). Infectious disease in an era of global change. Nature Reviews Microbiology, 20(4), 193–205. https://doi.org/10.1038/s41579-021-00639-z
- [7] Pragathi, P., Shetty, U., Parida, P., Varamballi, P., Mukhopadhyay, C., Sudheesh, N. (2024). Molecular detection and genotyping of HMPV in patients with severe acute respiratory infection in India. Annals of Medicine, 56(1). https://doi.org/10.1080/07853890.2024.2398719
- [8] Noffel, Z., Dobrovolny, H. M. (2024). Modeling the bystander effect during viral coinfection. Journal of Theoretical Biology, 594, 111928. https://doi.org/10.1016/J.JTBI.2024.111928
- [9] Devanathan, N., et al. (2025). Emerging lineages A2.2.1 and A2.2.2 of human metapneumovirus (hMPV) in pediatric respiratory infections: Insights from India. IJID Regions, 14, 100486. https://doi.org/10.1016/J.IJREGI.2024.100486
- [10] Zhu, R., et al. (2020). Epidemiological and genetic characteristics of human metapneumovirus in pediatric patients across six consecutive seasons in Beijing, China. International Journal of Infectious Diseases, 91, 137–142. https://doi. org/10.1016/J.IJID.2019.11.012
- [11] Pidjadee, C., Soh, K. L., Attharos, T., Soh, K. G. (2024). The effect of infection prevention and control programme for childcare workers in daycare centres: A systematic review. Journal of Pediatric Nursing, 79, 116–125. https://doi.org/10.1016/j.pedn.2024.09.002
- [12] Mendes Neto, A. G., et al. (2021). Bacterial infections and patterns of antibiotic use in patients with COVID-19. Journal of Medical Virology, 93(3), 1489–1495. https://doi.org/10.1002/JMV.26441
- [13] Nardo, D., Maddox, E. G., Riley, J. L. (2025). Cell therapies for viral diseases: A new frontier. Seminars in Immunopathology, 47(1), 1–8. https://doi.org/10.1007/S00281-024-01031-8
- [14] Motta, C. M., Keller, M. D., Bollard, C. M. (2023). Applications of virus-specific T cell therapies post-BMT. Seminars in Hematology, 60(1), 10–19. https://doi.org/10.1053/J.SEMINHEMATOL.2022.12.002
- [15] Feltes, T. F., et al. (2003). Palivizumab prophylaxis reduces hospitalization due to respiratory syncytial virus in young children with hemodynamically significant congenital heart disease. Journal of Pediatrics, 143(4), 532–540. https://doi.org/10.1067/S0022-3476(03)00454-2
- [16] Enver, A., Ayaz, F. (2025). Mathematical modeling of stress induced type 2 diabetes and atherosclerosis: Numerical methods and stability analysis. Results in Nonlinear Analysis, 8(1), 204–225. https://doi.org/10.31838/rna/2025.08.01.019
- [17] Nabti, A., Djilali, S., Bentout, S. (2025). Stability and spatial profiles of a double age-dependent diffusive viral infection model with spatial heterogeneity. Zeitschrift fur angewandte Mathematik und Physik, 76, 89. https://doi.org/10.1007/ s00033-025-02087-6
- [18] Bentout, S., Djilali, S. (2024). Asymptotic profiles of a generalized reaction-diffusion SIS epidemic model with spatial heterogeneity. Zeitschrift fur angewandte Mathematik und Physik, 75, 225. https://doi.org/10.1007/s00033-024-02025-3
- [19] Djilali, S., Sarmad, G., Tridane, A. (2025). Dynamics and asymptotic profiles of a local-nonlocal dispersal SIR epidemic model with spatial heterogeneity. Infectious Disease Modelling, 10(2), 387–409. https://doi.org/10.1016/j.idm.2025.03.007
- [20] Djilali, S., Chen, Y., Zou, S. (2025). A diffusive SIS epidemic model in a heterogeneous environment: Random dispersion vs. nonlocal dispersion. Mathematics and Computers in Simulation, 236, 90–110. https://doi.org/10.1016/j.matcom.2025.06.004
- [21] Enver, A., Ayaz, F., Yalcinkaya, D. E. (2025). A multiscale coupled reaction-diffusion model of amyloid-beta and tau pathology in Alzheimer's disease. Journal of Nonlinear Modeling and Analysis, 7(5), 1940–1964. https://doi. org/10.12150/jnma.2025.1940